p-ISSN : 2335-1357 e-ISSN : 2437-1122

Mediterranean Journal of Modeling and Simulation

Med. J. Model. Simul. 11 (2019) 020-035

Experimental potential of exploiting PEMFC's waste heat using TEG modules

B. Abderezzak [a] *, M. Hinaje [b] , J. Leveque [b]

[a] Laboratoire de l'Énergie et des Systèmes Intelligent (LESI), University of Khemis Miliana, Road of Theniet El Had, 44225, Khemis Miliana, Algeria

[b] Laboratoire GREEN, Faculté des Sciences et Technologies, Université de Lorraine, B.P. 70 239, Vandœuvre-lès-Nancy Cedex, 54 506, France

ARTICLE INFO

Article history :
Received May 2019
Accepted July 2019

Keywords :
PEM Fuel Cell ;
Thermoelectric Generators ;
Energy storage ;
Heat recovery ;
Seebeck coefficient.

ABSTRACT

This work is an experimental approach regarding the opportunity to exploit Proton Exchange Membrane Fuel Cell (PEMFC) waste heat, using Thermoelectric Generator (TEG) Modules. The amount of energy recovered by TEG modules can be stored using NiMH batteries, and used for feeding the PEMFC Stack screens and LED lights once its turns on "Stand-by" mode. In fact, several combinations are envisaged to depict the optimal working conditions of the proposed system. The proposed 6A and 15A TEG modules are experienced under a 20A and 30A of load applied on the PEMFC Stack. A Re-Start mode is then investigated to observe the system response against such scenarios. The experimental result shows a promising output voltage rates generated by the TEG modules. At stack working temperature of 60řC, the 15A TEG voltage is 500 mV and 571 mV under stack load of 20A and 30A respectively. In Re-Start mode, at same stack temperature, the output voltage is 517 mV.
A numerical approach is employed for the determination of experimental Seebeck coefficient and the evaluation of the thermoelectric conversion efficiency, using a one-dimensional (1-D) steady state model. A polynomial function of the experimental Seebeck coefficient is then deduced.

Nomenclature

Abbreviations	
PEMFC	Polymer Electrolyte Membrane Fuel Cell
TEG	Thermoelectric generator
I	Electrical Current [A]
V	Voltage [V]
R	Electrical resistance [Ohm]

*Email : b.abderezzak@univ-dbkm.dz

P	Electrical power [W]
Q	Heat flow [W]
T	Temperature [K]
k	Thermal conductivity [W/mK]
K	Thermal transfer coefficient [W/m^{2}K]
N	Junction number
Z	Figure of merit

Greek letter

ρ	Electrical resistivity [Ohm . m]
η	Efficiency
α	Seebeck coefficient

Superscripts and subscripts

j	joule heating
n	n-type semiconductor
p	p-type semiconductor
c	cold
h	hot
$ceram$	ceramic plate
cp	copper tabs
i	internal
e	external
L	Load
k	conduction

1. Introduction

Climate change problem is closely related to the atmospheric pollution sources, which is a consequence of our daily use of power and heat generated from fossil fuels. The increase of greenhouse gases emissions lead to think about the development of new solutions to fight, to brake or even to slow down the global warming phenomena. Among the proposed solutions is the development of alternative efficient energy generation systems, with large consideration to the environment-friendly aspects. Several alternative energy generation systems exist under the name of green and renewable energy. In fact, some technologies were developed as well as solar thermal, solar photovoltaic panels, wind turbines, hydraulic, marine and geothermal power plants. Energy can also be stored under an energy carrier such as hydrogen to be reused through fuel cells. In order to enhance the efficiency of some green energy generation systems, the waste heat is then recovered.

Recent research works [1-9] deal with the possibility to exploit free, sustainable and environment – friendly heat sources, such as solar and geothermal sources. Other research works focus on the opportunity to benefit from rejected heat of existing systems as well as boilers, furnaces, wood cookers, automobile gas exhaust or even fuel cells.

Thermoelectric technology offers the possibility to employ waste heat for power generation ; it is a cost-effective source due to its availability and environment friendly as

well. Demir et al. [10] proposed a novel hybrid system composed of a Solar thermal, TEG modules and a PEM Electrolyzer, to generate electricity, fresh water and hydrogen. They implemented a phase change material to avoid water production fluctuation. Result shows a TEG modules contribution in the amount of produced electricity by 6.8 % thanks to the waste heat recovering strategy. Hydrogen production increased by 19.1 % while increasing the operating temperature.

Recently, Shu et al. [11], developed a 3D numerical model of segmented TEG modules integrated on the engine exhaust system. A comparison between two configurations of the modules leads to increase output power by 13.4 % while using thinner exchanger with multi modules structure to be 78.9 W. More result shows also that fins can alter the optimal configuration of the modules, the output power is then estimated to be 89.7 W.

Hasani et al. [12] investigated the performances of thermoelectric cooler modules connected with heat exchanger working with water as thermal fluid, a heat sink and a waste heat recovered from a 5 kW PEM Fuel Cell. Their experimental result shows a constant value of 0.04% in the performance of the modules with water temperature beyond 50°C. They presented also a new correlation to estimate the open circuit voltage in terms of water inlet temperature.

In the work of Kwan et al. [13], a Cogeneration Heat and Power scenario using Fuel Cells is compared with a coupled Thermoelectric – Fuel cells device. The analysis is performed under exergetic and temperature aspects, while a steady state models for both scenarios are developed and compared. Result shows the enhanced value of the exergetic efficiency by up to 2% in the thermoelectric scenario, and recommended values of water flow and fan speed are set.

Gao et al. [14] developed a numerical model of TEG modules closely connected to a High Temperature PEMFC via a compact plate–fin heat exchanger. The optimized configuration of the heat recovery system is found thanks to discretized model. The heat transfer process and the fluid properties were also discussed.

In this work, authors aim to experience a PEMFC – TEG system for supplementary power generation. PEMFC has a 1 kW power generated from hydrogen and air, with auto-humidification option. However, the amount of waste heat is also 1 kW, which justify the environment-friendly heat source. The TEG modules are set with direct contact to bipolar plates using Silicone free thermal grease. The amount of energy recovered by TEG modules can be stored using NiMH batteries, and used for feeding the PEMFC Stack screens and LED lights once its turns on "Stand-by" mode. A numerical model is then conducted to evaluate theoretically the amount of heat recovered from the PEMFC stack and the amount of power generated thanks to the TEG module, the experimental Seebeck coefficient is then deduced and an experimental polynomial function is set.

2. Thermoelectric technology description

Thermoelectric Generators are technical devices composed of semi-conductor materials connected with copper junctions. It can be found usually under small dimensions (40 x 40 x 3) mm, it is used to generate voltage while a thermal flux, (heat source), is applied on one side, and a heat sink from the other side. A thermoelectric generator device is structured as well as illustrated in Fig.1.

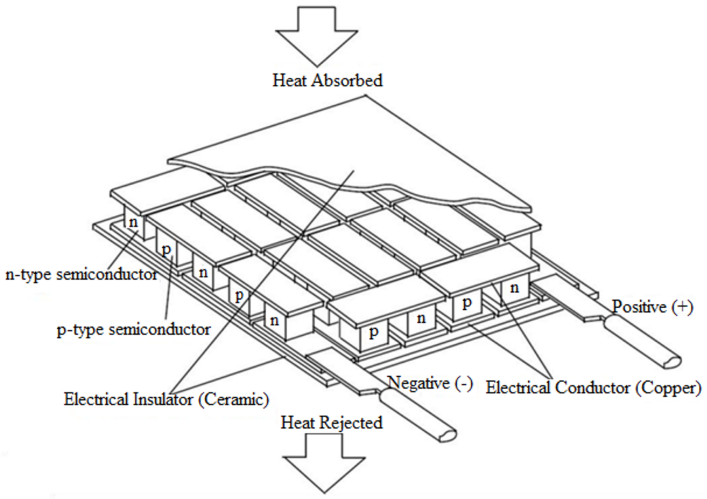

Fig. 1 – Components of a conventional thermoelectric module

A thermoelectric generator module is composed of a certain number of slabs called (legs), essentially made of p-type and n-type semiconductors forming thermocouples. All the legs are electrically connected in series through conductive copper tabs, and thermally connected in parallel. Two ceramic plates come to sandwich the legs and copper strips from top and from bottom as well as shown in Fig.2. The role of ceramic plate is to conduct heat and to insulate current in the same time.

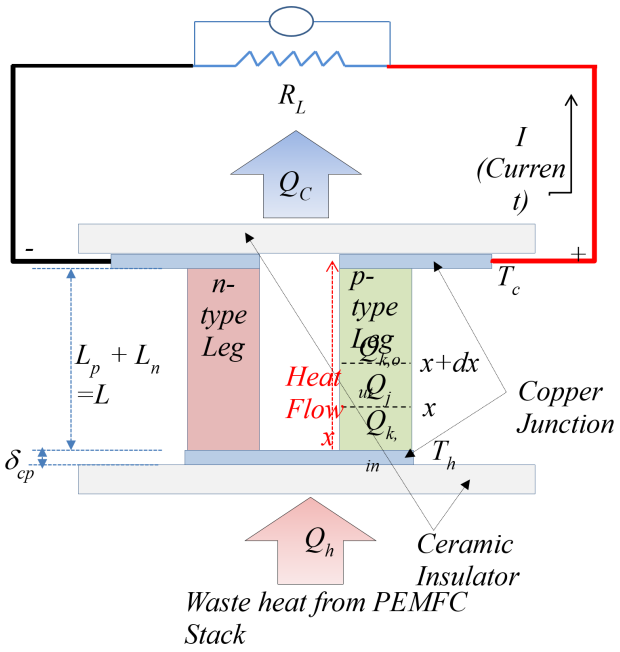

Fig. 2 – Schematic of p-type and n-type disposition

The use of thermoelectric generator device presents important advantages compared to other power generation systems. They are silent working and less cumbersome, it possesses no moving parts and no liquid state or phase change fluids while converting heat into power. In addition, TEG devices have a long lifetime compared to other similar technologies.

The working principle of a TEG module follows four main interdependent effects described below.

2.1. Four effects for one technology

Thermoelectric technology consists firstly of Seebeck effect which describes the induction of voltage, while two different material's junction is maintained at different temperatures ; it can be increased as well temperature difference increase.

In second position comes the Peltier effect which describes thermal energy absorption or dissipation at the connection of two conducting materials with a current flow through this junction. The thermal energy, heat, is the then absorbed or dissipated following the direction of current flow.

The Thomson effect is also present in this technology ; it consists on the absorption or dissipation of thermal energy when electric current flows through a circuit composed of single material ; with a moderate temperature variation along its length.

Finally, the joule heating effect manifests itself by the material's thermal energy dissipation with the presence of electrical resistance and electrical current.

2.2. Thermoelectric generator (TEG) module calculations

To find scientific description of the heat-to-power behavior of a thermoelectric generator module, the best is to follow a one-dimensional (1-D) steady state theoretical model based on the conservation of energy. Referring to Fig. 2, the p-type leg heat flow can be divided into three main thermal transfer : (i) heat transferred by conduction from hot side noted ($Q_{k,in}$), (ii) heat generated by the joule heating noted (Q_j) and (iii) the heat transferred by conduction out of the p-type leg noted ($Q_{k,out}$), [15]. The first energy conservation equation leads to :

$$Q_{k,in} - Q_{k,out} + Q_j = 0 \tag{1}$$

Working with a differential control volume inside of p-type semiconductor leg gives the following expression of the energy equation :

$$Q\left(x\right) - Q\left(x + dx\right) + Q_j = 0 \tag{2}$$

After using the Taylor expansion, the previous equation becomes :

$$Q\left(x\right) - \left(Q\left(x\right) + \frac{\partial Q\left(x\right)}{\partial x} dx\right) + \frac{I^2 \rho_p}{A_p} dx = 0 \tag{3}$$

After simplifications, and with consideration to the Fourier's law of conduction for one-dimensional steady state condition, the previous equation takes the following form :

$$k_p A_p \frac{d^2 T_p}{dx^2} dx + \frac{I^2 \rho_p}{A_p} dx = 0 \tag{4}$$

The integral form of this equation gives :

$$\int_0^x k_p A_p \frac{d^2 T_p}{dx^2} dx + \int_0^x \frac{I^2 \rho_p}{A_p} dx = 0 \tag{5}$$

After integration, the following equation is found :

$$k_p A_p \left(\frac{dT_p}{dx}|_x - \frac{dT_p}{dx}|_0 \right) + \frac{I^2 \rho_p}{A_p} x = 0 \tag{6}$$

Using the boundary conditions for resolving this equation gives :

$$x = 0 \ \rightarrow \ T_p(0) = T_h \tag{7}$$

Then

$$k_p A_p \frac{dT_p}{dx}|_0 = Q_p(0) \tag{8}$$

T heat transferred by conduction in the p-type leg is then $Q_p(0)$, the following equation is obtained :

$$\int_0^{L_p} k_p A_p \frac{dT_p}{dx} dx + \int_0^{L_p} \frac{I^2 \rho_p}{A_p} x dx = -\int_0^{L_p} Q_p(0)\, dx \tag{9}$$

After integrating, the equation becomes :

$$k_p A_p \left(T_p(L_p) - T_p(0) \right) + \frac{I^2 \rho_p}{A_p} \frac{L_p^2}{2} = -Q_p(0) L_p \tag{10}$$

Considering again the following boundary conditions :

$$x = 0 \ \rightarrow \ T_p(0) = T_h \tag{11}$$

And

$$x = L_p \ \rightarrow \ T_p(L_p) = T_c \tag{12}$$

The Fourier heat conduction equation becomes :

$$Q_p(0) = \frac{k_p A_p}{L_p} (T_h - T_c) - \frac{1}{2} \frac{\rho_p L_p}{A_p} I^2 \tag{13}$$

The heat balance in steady state in the hot side at T_h can be expressed as follows :

$$Q_h = Q_{p,h} + Q_{n,h} \tag{14}$$

Where $Q_{p,h}$ and $Q_{n,h}$ are p-type and n-type heat flows absorbed respectively at the hot junction, they can be defined with the Peltier Heat, the Joule Heating and the Fourier's law of conduction as follows :

$$Q_{p,h} = \alpha_p I T_h - \frac{1}{2}\frac{\rho_p L_p}{A_p} I^2 + \frac{k_p A_p}{L_p}(T_h - T_c) \tag{15}$$

And

$$Q_{n,h} = -\alpha_n I T_h - \frac{1}{2}\frac{\rho_n L_n}{A_n} I^2 + \frac{k_n A_n}{L_n}(T_h - T_c) \tag{16}$$

Where A, k, L and ρ are respectively the cross sectional area, thermal conductivity, length and electrical resistivity of p-type and n-type semiconductor legs, the heat balance at hot side becomes :

$$Q_h = (\alpha_p - \alpha_n) I T_h - \frac{1}{2}\left(\frac{\rho_p L_p}{A_p} + \frac{\rho_n L_n}{A_n}\right) I^2 + \left(\frac{k_p A_p}{L_p} + \frac{k_n A_n}{L_n}\right)(T_h - T_c) \tag{17}$$

The expression of the heat rejected at the cold junction of p-type and n-type legs can be derived using the same previous method. The following expression is obtained :

$$Q_c = (\alpha_p - \alpha_n) I T_c - \frac{1}{2}\left(\frac{\rho_p L_p}{A_p} + \frac{\rho_n L_n}{A_n}\right) I^2 + \left(\frac{k_p A_p}{L_p} + \frac{k_n A_n}{L_n}\right)(T_h - T_c) \tag{18}$$

As it can be observed, the thermoelectric generator is function of heat absorbed from the hot side and that rejected on the cold side, the flow of current in the electrical circuit with load resistor, the induced voltage and power output. For more simple form of the two previous equations, a suggestion has been made as follows :

- For Seebeck coefficient

$$\alpha = \alpha_p - \alpha_n \tag{19}$$

- For electrical resistance

$$R = \frac{\rho_p L_p}{A_p} + \frac{\rho_n L_n}{A_n} \tag{20}$$

- And for thermal conductance :

$$K = \frac{k_p A_p}{L_p} + \frac{k_n A_n}{L_n} \tag{21}$$

For N number of semiconductor thermocouples, the expressions of heat flows through respectively the hot and the cold junction becomes :

$$Q_h = N\left[\alpha I T_h - \frac{1}{2} R I^2 + K(T_h - T_c)\right] \tag{22}$$

And

$$Q_c = N\left[\alpha I T_c + \frac{1}{2} R I^2 + K(T_h - T_c)\right] \tag{23}$$

The difference between the absorbed and rejected heat at hot and cold junction respectively, seems to be the best approximation of the power generated, the expression becomes :

$$P = Q_h - Q_c = N\left[\alpha I\left(T_h - T_c\right) - RI\right] \tag{24}$$

The first derivation of the previous power expression leads to the optimal current generated form, after first derivation with respect to the current, the following expression is obtained :

$$\frac{dP}{dI} = N\left[\alpha\left(T_h - T_c\right) - 2RI\right] \tag{25}$$

The expression of the optimal current is then obtained by equating the previous equation to zero, it becomes :

$$I_{opt} = \frac{\alpha\left(T_h - T_c\right)}{2R} \tag{26}$$

The current, the output power and voltage induced in the thermoelectric generators can be reorganized as the following combination of thermocouples presented in Fig.2.

This configuration has a close dependence with the external resistance load noted RL, the expressions of the current, output power and voltage induced becomes :

$$I = \frac{\alpha\left(T_h - T_c\right)}{R + R_L} \tag{27}$$

And

$$P = R_L I^2 = R_L\left(\frac{\alpha\left(T_h - T_c\right)}{R + R_L}\right)^2 \tag{28}$$

And

$$V = R_L I = R_L\left(\frac{\alpha\left(T_h - T_c\right)}{R + R_L}\right) \tag{29}$$

As an optimization, R_L needs to be equal the p-type and n-type total internal electrical resistance of the semiconductor legs. At this stage, the thermoelectric generator efficiency can be easily defined as :

$$\eta = \frac{P}{Q_h} \tag{30}$$

The maximum efficiency delivered by the thermoelectric generator is function of the figure of merit parameter Z of both p-type and n-type semiconductors, and the average temperature between hot and cold sides $\bar{T}$, it is expressed as follows :

$$\eta_{max} = \left(1 - \frac{T_h}{T_c}\right) \frac{\sqrt{1 + Z\bar{T}} - 1}{\sqrt{1 + Z\bar{T}} + \frac{T_h}{T_c}} \tag{31}$$

The figure of merit Z characterizes the thermoelectric materials of p-type and n-type semiconductor legs. It gives an approximation about the ability of the thermoelectric materials to convert heat into electrical power. It is generally expressed as follows :

$$Z = \frac{\alpha^2}{\rho\, k} \tag{32}$$

When designing TEG's, the semiconductor leg geometry and the thermoelectric material properties must satisfy the following equation in order to enhance the figure of merit :

$$\frac{A_p^2 L_n^2}{A_n^2 L_p^2} = \frac{k_n \rho_p}{k_p \rho_n} \tag{33}$$

For technical and economical manufacturing considerations, p-type and n-type semiconductor legs should be with the same geometry. Moreover, the thermoelectric properties should be the same. In general, the best thermoelectric material should have low electrical resistivity and low thermal conductivity while it needs a higher Seebeck coefficient.

2.3. Equivalent thermal resistance network

The Thermoelectric generator module is presented in Fig.1 and zoomed with details in Fig.2, represents a heat transfer area composed of connected layers : p-type and n-type semiconductor legs, copper strips, ceramic plates, thermal grease, heat sink and fans. These layers are described in Fig. 3. A better described thermal network helps to determine the heat transfer rate through these previous layers. A complete temperature level of the thermal resistance network for the employed TEG module is presented in Fig. 4.

Where :

$R_{ceram,h}$, $R_{ceram,c}$: Ceramic plate thermal resistance respectively for hot and cold side,

$T_{i,ceram,h}$, $T_{e,ceram,h}$, $T_{i,ceram,c}$, $T_{e,ceram,c}$:Internal and external temperatures of hot and cold ceramic plate respectively,

T_h, T_c : Temperature of respectively hot and cold junction (p-type and n-type legs),

T_{amb} : Ambient temperature,

$R_{cp,h}$, $R_{cp,c}$: Thermal resistance of copper strip at respectively hot and cold side,

R_{leg} : Thermal resistance of semiconductor legs (p-type and n-type),

R_{amb} : Ambient air thermal resistance under forced convection.

R_{TG} :Thermal grease resistance

3. The PEMFC-TEG experimental approach

As well as presented in Fig. 3 and Fig. 4, a silicone free thermal grease is used to fix the 12715 and 12706 thermoelectric module on the top of the bipolar plate of a 1 kW PEM Fuel Cell fed by pure hydrogen and humidified air.

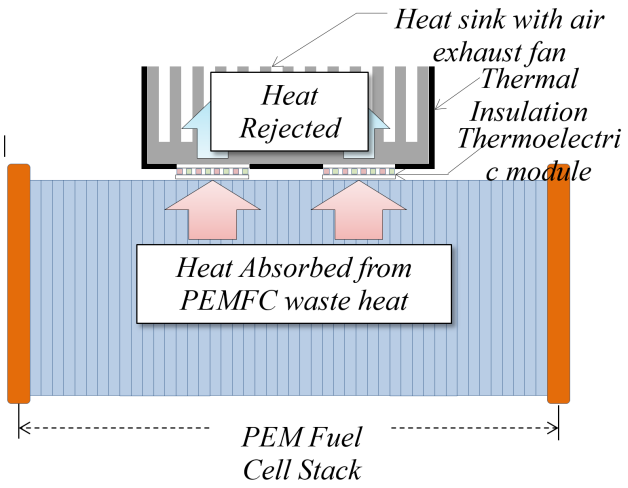

Fig. 3 – Schematic of the experienced PEMFC-TEG system

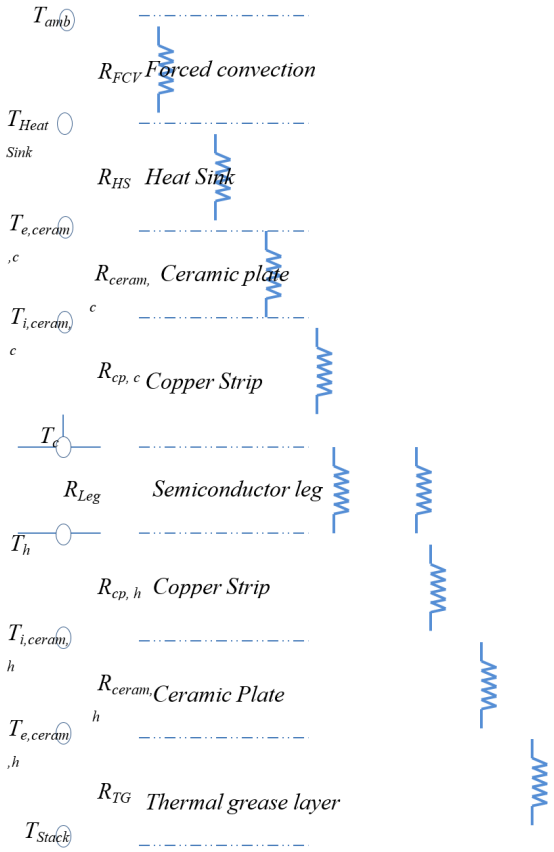

Fig. 4 – Equivalent thermal resistance network

The experimental work is presented in Fig. 5 and Fig. 6 ; it follows three main steps : (i) TEG packaging with heat sink and thermal insulation, (ii) PEMFC-TEG fixation and (iii) Electrical and data acquisition connections. Table 1 summarizes the TEG package elements properties.

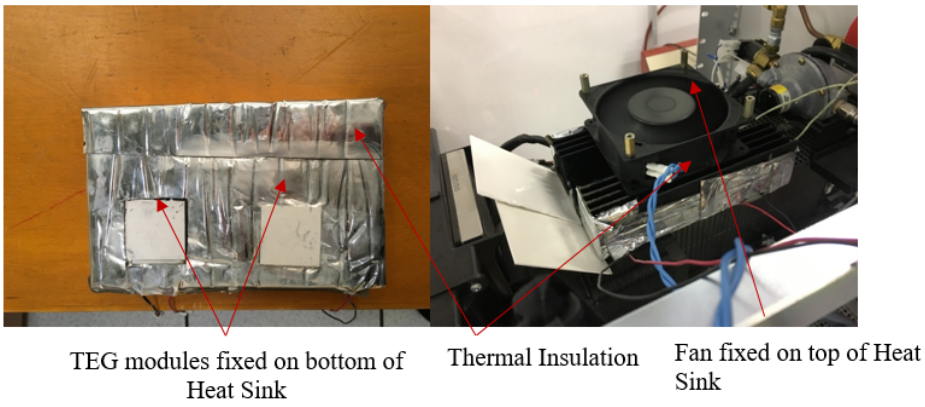

Fig. 5 – Preparation of the PEMFC-TEG experimental approach

The general view of the experimental work is summarized in the following figure 6.

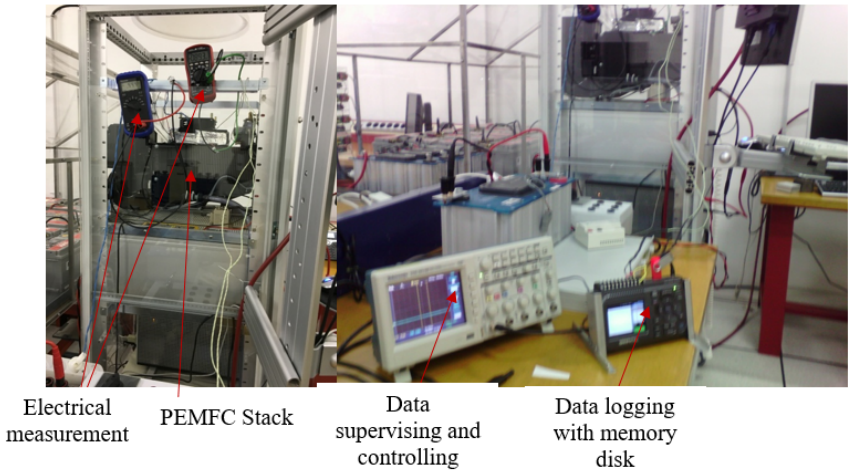

Fig. 6 – Electrical and data connections

And the thermoelectric module properties are illustrated in Table 1 :

Table 1 – TEG module package Elements properties

Elements	**Properties**
Heat sink	Aluminium (30 x 15 x 8)
TEC 12706	127 junction supporting up to 6 Amps
TEC 12715	127 junction supporting up to 15 Amps
Extraction fan	Φ=10 cm ; P=15 W
Thermal insulation	Adhesive polyurethane insulator

For the calculations, authors preferred to use the following real values of semiconductors and geometry.

Table 2 – TEG semiconductor values and geometry

Elements	Values
$\rho_n = \rho_p$	1 x 10^{-5} Ω. m
$A_n = A_p$	0.41 x 0.41 .10^{-6} m^2
$L_n = L_p$	2 x 10^{-3} m
$k_n = k_p$	1.6 W/mK

3.1. The experimental process and results

In order to explore the existing potential of exploiting waste heat from PEMFC into power via a proposed TEG package, authors lunched an experimental campaign. Three scenarios are envisaged : (i) PEMFC stack under a load of 20 A, (ii) PEMFC stack under load of 30 A and (iii) PEMFC stack under 30A with Re-start mode after shut-down period. Both thermoelectric modules (6A and 15 A) are experienced; data are supervised in real time, and collected for display purpose. Experimental Result in Fig. 7 and Fig. 8 shows a non-negligible voltage delivered from the 6A TEG module and much more important for that generated from 15A TEG module.

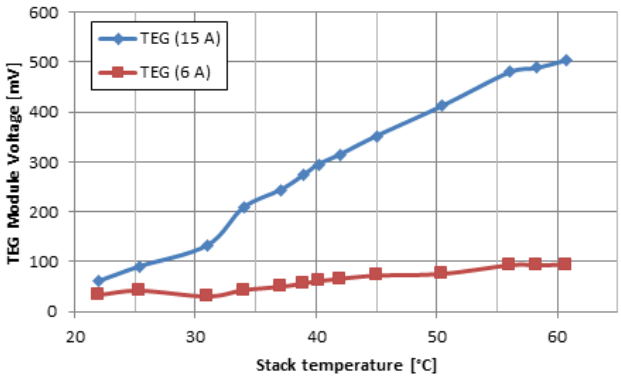

Fig. 7 – Voltage generated under 20A load for PEMFC Stack

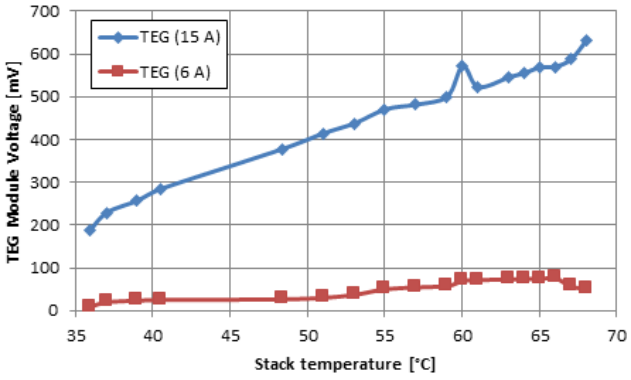

Fig. 8 – Voltage generated under 30A load for PEMFC Stack

For the 6A TEG module, the evolution in the generated voltage is from 32mV to 94 mV while stack temperature vary from 22°C to 61°C. For the same temperature range,

but in the case of 15A TEG module, the evolution is more important, it vary from 60mV to 505mV.

The cold side of the TEG temperature is maintained at ambient temperature thanks to the conduction and forced convection heat transfer, the evolution of this temperature during the experiment running time is presented in Fig. 9.

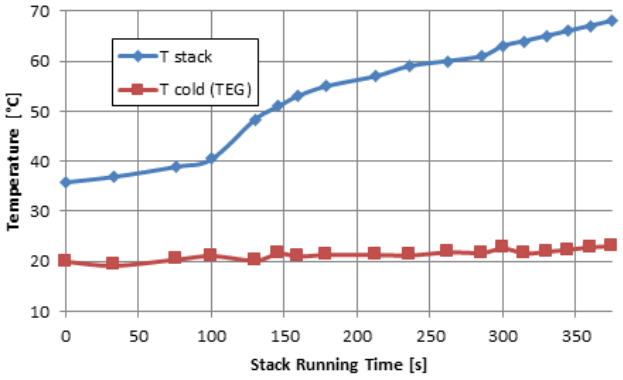

Fig. 9 – Comparison between stack temperature and TEG cold side (30A load)

In fact, the huge dimension of the aluminum made heat sink compared to the TEG dimensions is very useful for quick and effective heat extraction.

After 15 minutes shut-down of the stack, authors experienced the Re-start mode, results are drawn in Fig. 10.

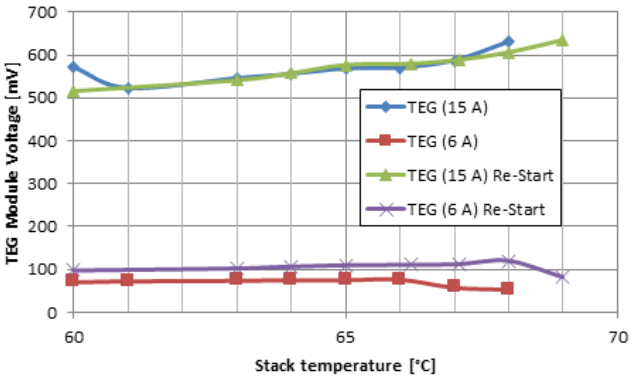

Fig. 10 – Voltage generated under 30A load for PEMFC Stack with Re-start mode

According to these results, a small gain is observed in voltage in the Re-start mode for both 6A and 15A TEG, it is mainly due to the pre-heated phase of the PEMFC stack, the running time is then shortened.

3.2. Experimental determination of Seebeck Coefficient

As known, Seebeck coefficient describes the rate to transform heat into power ; however it is unknown in this experimental approach which conducts authors to an experimental characterization. Following the previous one-dimensional (1-D) model, the seebeck coefficient can be deduced experimentally with consideration to hot side temperature taken as

the stack temperature, and the cold side temperature taken as contact temperature between heat sink and TEG module. Table 2 summarizes the values of employed parameters.

In addition, the generated voltage is the third known parameter for this experimental determination, the following graphic illustrated in Fig. 11 is then developed.

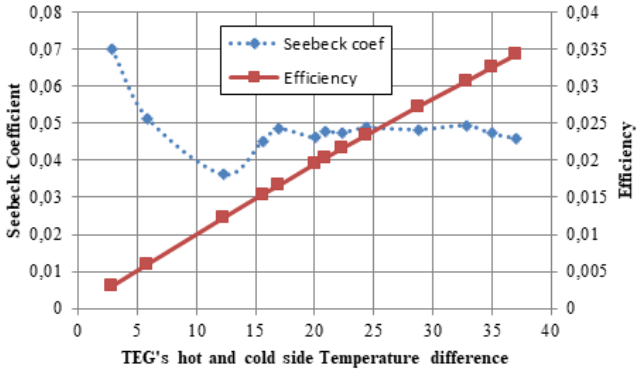

Fig. 11 – Efficiency and experimental Seebeck Coefficient

From this figure, we can observe the close dependence of Seebeck coefficient to the temperature difference between cold and hot side. A stable value of 0.5 is then observed.

Numerically speaking, a polynomial function of Seebeck coefficient with temperature difference is then sorted from the experimental evolution as follows :

$$\alpha = 3 \times 10^{-5} \cdot \Delta T^2 - 0.0017 \cdot \Delta T + 0,0651 \tag{34}$$

The thermoelectric conversion efficiency is also drawn in the same previous figure, it represents a linear evolution to attend the value of 0.035 % with temperature difference of 40°C, this matches approximately the value of 60°C in the stack temperature.

4. Conclusions and future works

This research work is based on both numerical and experimental approach of a coupled PEMFC-TEG system. The main purpose is to exploit the existing waste heat into power thanks to thermoelectric generators modules. The amount of voltage generated is important in the case of the 15A thermoelectric generator module. The experience is then remade under Re-start mode, and a small gain in the generated voltage is observed. The heat sink temperature is memorized during the running time of the experience, the utilization of big dimensions with finned aluminum heat sink and forced convection leads to a stable cold side temperature. A numerical approach is employed for the determination of experimental Seebeck coefficient and the evaluation of the thermoelectric conversion efficiency.

The generated voltage is very valuable when used for energy storage using NiMH batteries, and reused for feeding the PEMFC Stack screens and LED lights once its turns on "Stand-by" mode. Future work deals with the concretization of such system.

Acknowledgment

I hereby thanks the Green Laboratory to give me the opportunity to deal with Fuel Cells facilities and for their support regarding the acquisition of thermoelectric modules and success this work. Another thanks is dedicated to the Lesi laboratory for the financial support of the mobility under Khemis Miliana Grant responsibility.

REFERENCES

[1] D. Jiang, Z. Fan, M. Dong, Y. Shang, X. Liu, G. Chen, S. Li. Titanium nitride selective absorber enhanced solar thermoelectric generator (SA-STEG), Applied Thermal Engineering, Volume 141, 2018, Pages 828-834.

[2] G. Omer, A. H. Yavuz, R. Ahiska. Heat pipes thermoelectric solar collectors for energy applications, International Journal of Hydrogen Energy, Volume 42, Issue 12, 2017, Pages 8310-8313.

[3] H. Hazama, Y. Masuoka, A. Suzumura, M. Matsubara, S. Tajima, R. Asahi. Cylindrical thermoelectric generator with water heating system for high solar energy conversion efficiency, Applied Energy, Volume 226, 2018, Pages 381-388.

[4] S. Thongsan, B. Prasit, T. Suriwrong, Y. Mensin, W. Wansungnern. Development of solar collector combined with thermoelectric module for solar drying technology, Energy Procedia,Volume 138, 2017, Pages 1196-1201.

[5] Y.S. Jung, D.H. Jeong, S.B. Kang, F. Kim, M.H. Jeong, K.S. Lee, J.S. Son, J.M. Baik, J.S. Kim, K.J. Choi. Wearable solar thermoelectric generator driven by unprecedentedly high temperature difference, Nano Energy, Volume 40, 2017, Pages 663-672.

[6] L.C. Ding, A. Akbarzadeh, L. Tan. A review of power generation with thermoelectric system and its alternative with solar ponds, Renewable and Sustainable Energy Reviews, Volume 81, Part 1, 2018, Pages 799-812.

[7] Dongfang Sun, Limei Shen, Yu Yao, Huanxin Chen, Shiping Jin, Hong He.The real-time study of solar thermoelectric generator, Applied Thermal Engineering, Volume 119, 2017, Pages 347-359.

[8] S. Mahmoudinezhad, A. Rezania, L.A. Rosendahl, Behavior of hybrid concentrated photovoltaic-thermoelectric generator under variable solar radiation, Energy Conversion and Management, Volume 164, 2018, Pages 443-452.

[9] R. Lamba, S.C. Kaushik. Solar driven concentrated photovoltaic-thermoelectric hybrid system : Numerical analysis and optimization, Energy Conversion and Management, Volume 170, 2018, Pages 34-49.

[10] M.E. Demir, I. Dincer, Development of a hybrid solar thermal system with TEG and PEM electrolyzer for hydrogen and power production, International Journal of Hydrogen Energy, Volume 42, Issue 51, 2017, Pages 30044-30056.

[11] G. Shu, X. Ma, H. Tian, H. Yang, T. Chen, X. Li. Configuration optimization of the segmented modules in an exhaust-based thermoelectric generator for engine waste heat recovery, Energy, Volume 160, 2018, Pages 612-624.

[12] M. Hasani, N. Rahbar. Application of thermoelectric cooler as a power generator in waste heat recovery from a PEM fuel cell – An experimental study, International Journal of Hydrogen Energy, Volume 40, Issue 43, 2015, Pages 15040-15051.

[13] T.H. Kwan, Q. Yao. Exergetic and temperature analysis of a fuel cell-thermoelectric device hybrid system for the combined heat and power application, Energy Conversion and Management, Volume 173, 2018, Pages 1-14.

[14] X. Gao, S. J. Andreasen, M.C. S.K. Kær. Numerical model of a thermoelectric generator with compact plate-fin heat exchanger for high temperature PEM fuel cell exhaust heat recovery, International Journal of Hydrogen Energy,Volume 37, Issue 10, 2012, Pages 8490-8498.
[15] D.M. Rowe. CRC handbook of thermoelectric, CRC press, Boca Raton, 1995.